Systems/Circuits

Organization of Corollary Discharge Neurons in Monkey Medial Dorsal Thalamus

James Cavanaugh, Kerry McAlonan, and Robert H. Wurtz
Laboratory of Sensorimotor Research, National Eye Institute, National Institutes of Health, Bethesda, Maryland 20892

A corollary discharge (CD) is a copy of a neuronal command for movement sent to other brain regions to inform them of the impending movement. In monkeys, a circuit from superior colliculus (SC) through medial-dorsal nucleus of the thalamus (MD) to frontal eye field (FEF) carries such a CD for saccadic eye movements. This circuit provides the clearest example of such internal monitoring reaching cerebral cortex. In this report we first investigated the functional organization of the critical MD relay by systematically recording neurons within a grid of penetrations. In two male rhesus macaque monkeys (*Macaca mulatta*), we found that lateral MD neurons carrying CD signals discharged before saccades to ipsilateral as well as contralateral visual fields instead of just contralateral fields, often had activity over large movement fields, and had activity from both central and peripheral visual fields. Each of these characteristics has been found in FEF, but these findings indicate that these characteristics are already present in the thalamus. These characteristics show that the MD thalamic relay is not passive but instead assembles inputs from the SC before transmission to cortex. We next determined the exact location of the saccade-related CD neurons using the grid of penetrations. The neurons occupy an anterior-posterior band at the lateral edge of MD, and we established this band in stereotaxic coordinates to facilitate future study of CD neurons. These observations reveal both the organizational features of the internal CD signals within the thalamus, and the location of the thalamic relay for those signals.

Key words: **corollary discharge; macaque; MD; thalamus**

Significance Statement

A corollary discharge (CD) circuit within the brain keeps an internal record of physical movements. In monkeys and humans, one such CD keeps track of rapid eye movements, and in monkeys, a circuit carrying this CD extends from midbrain to cerebral cortex through a relay in the thalamus. This circuit provides guidance for eye movements, contributes to stable visual perception, and when defective, might be related to difficulties that schizophrenic patients have in recognizing their own movements. This report facilitates the comparison of the circuit in monkeys and humans, particularly for comparison of the location of the thalamic relay in monkeys and in humans.

Introduction

A brain circuit extending from the superior colliculus (SC) through the medial-dorsal nucleus of the thalamus (MD) to the frontal eye field (FEF) carries copies of the motor commands producing saccadic eye movements: a corollary discharge (CD; for review, see Sommer and Wurtz, 2008; Wurtz, 2008, 2018). This circuit provides the clearest example of internally generated brain signals that act on visual processing in cerebral cortex.

Single neuron recordings and transient inactivations in the relay within MD thalamus have established that this circuit conveys a CD to cerebral cortex. Neurons in lateral MD discharge before saccades, as do neurons in intermediate layers of SC, from which they receive input (Sommer and Wurtz, 2002, 2004a), as would be expected of a CD. Inactivations of MD break the connection between SC and FEF and provide critical evidence that these neurons convey a CD that affects behavior. The double saccade task (Hallett and Lightstone, 1976) is used as an assay for CD because the accuracy of the second saccade, made in the absence of a visual target, is dependent on the CD. Inactivation of lateral MD changes the CD-dependent second saccade but has little effect on the visually guided first saccade (Sommer and Wurtz, 2002, 2004b). MD inactivations provide strong evidence that saccadic activity in MD is not driving saccades but instead is a CD copy of the SC activity that drives saccades.

Received Sep. 30, 2019; revised Mar. 9, 2020; accepted May 26, 2020.

Author contributions: J.C., K.M., and R.H.W. designed research; J.C. and K.M. performed research; J.C. analyzed data; J.C. and R.H.W. wrote the paper.

This work was supported by the National Eye Institute Intramural Research Program at the National Institutes of Health.

The authors declare no competing financial interests.

Acknowledgements: We thank Altah Nichols, Tom Ruffner, and Daniel Yochelson for machine shop support.

Correspondence should be addressed to James Cavanaugh at jrc@lsr.nei.nih.gov.

https://doi.org/10.1523/JNEUROSCI.2344-19.2020

In this report, we address two substantial questions about CD neurons in MD. The first is that CD neurons in MD exhibit activity that crosses the visual vertical meridian. Jones (2007; p 147) stated succinctly: "Probably just about every nucleus of the dorsal thalamus has been attacked anatomically over the last 30 years and the weight of evidence from these studies is against connections joining together dorsal thalamic nuclei." The consequence of this is that each half of the thalamus has been regarded as related to the contralateral visual field. Initial experiments on the saccadic CD in lateral MD were consistent with this view; thalamic CD relay neurons were identified as receiving orthodromic input from the ipsilateral SC and projecting to the ipsilateral FEF, with activity centered in the contralateral visual field. (Sommer and Wurtz, 2004a). Recent inactivation experiments of lateral MD, however, showed that CD inactivation on one side of the thalamus produced a behaviorally measured perceptual deficit in both the contralateral and the ipsilateral visual fields. (Cavanaugh et al., 2016). Our first goal was to determine whether CD relay neurons in lateral MD also discharged with saccades to targets in both ipsilateral and contralateral visual hemifields. Does one side of the thalamus represent both visual fields despite minimal direct connections between the two sides? This would distinguish thalamic relay neurons carrying information internal to the brain from those carrying external sensory input or motor output (Sherman and Guillery, 1996).

The second question is more fundamental: where exactly are the CD neurons within MD? The current estimate of location was based on recording the saccade-related activity of MD neurons and the consequences of their inactivation (Sommer and Wurtz, 2002, 2004a,b; Cavanaugh et al., 2016). Estimated location was subservient to the sampling needed to do the specific experiments. In the present experiments, we made a systematic series of penetrations covering the relevant regions of lateral MD. This meticulous localization of the CD pathway to FEF allows a better comparison to the same pathway recently demonstrated in humans using diffusion tensor imaging (Yao et al., 2019). This monkey-to-human comparison has additional significance given the recently recognized similarity between the behavior of monkeys with inactivations of the CD in MD (Sommer and Wurtz, 2008) and difficulty of schizophrenic patients in identifying the origin of their actions (Thakkar et al., 2017; Bansal et al., 2018), comparisons that are considered in the discussion.

Materials and Methods

Experimental design and statistical analysis

Two adult male rhesus monkeys (*Macaca mulatta*, monkeys C and W), both weighing between 9 and 10 kg, were implanted with scleral search coils for measuring eye position, a post for immobilizing the head during experiments, and a recording cylinder to record from, and inactivate, regions of the thalamus. The recording cylinder was oriented in the stereotaxic vertical, and centered on the midline. Details of these procedures, including methods of training on the psychophysical task, are described in Joiner et al. (2013). All procedures were approved by the Institute Animal Care and Use Committee and complied with Public Health Service Policy on the humane care and use of laboratory animals.

In the dark, monkeys fixated on a laser spot back projected onto the center of a screen in front of them. During fixation another laser spot, the saccade target, was also projected on to the screen. The target appeared at a random location (almost always one of 25 locations in a 5×5 grid), with grid locations typically separated by 10° both horizontally and vertically. The target grid straddled the vertical meridian, but its center was placed (usually 5°) in the contralateral visual hemifield (see Figs. 1–3). This arrangement allowed us to determine whether the MD saccadic movement fields and visual receptive fields were represented in the ipsilateral hemifield. The target grid almost invariably extended 20° into the upper and lower visual fields. Only a few experiments varied from the typical target configuration.

Eye position was sampled at 1000 Hz. At the start of each trial, monkeys were required to be within a 1.5° square around the fixation point. After 500 ms of fixation, a laser spot appeared at one of the possible target locations, selected pseudorandomly. After a period of 500–1000 ms, the fixation spot went off, signaling the monkey to make a saccade to the target. The start of the monkey's saccade was determined during each trial as the time the monkey's eye position deviated 1.5° from fixation. Offline, more precisely, saccade initiation was identified as the time that eye velocity and acceleration both exceed 100°/s and 5000°/s^2, respectively. The monkey was rewarded if the saccade ended within a virtual 5° box centered on the target location (10° box for experiments exploring the visual field periphery). Only rewarded trials for correct saccades were included in the analysis.

We measured the mean activity of MD neurons (102 in monkey C, 39 in monkey O) within several different time epochs. The baseline activity for each neuron was the mean firing rate over all trials during fixation 100 ms before target onset. Visual responses and saccadic activity were calculated within time windows determined for each neuron. Significant neuronal activity was that which exceeded baseline by 3 SD of the baseline activity.

Significances of activity metrics were determined with the Wilcoxon signed-rank test using MATLAB (MathWorks). Calculation of neuronal activities and organization and interpolation of neuronal data (as explained below) were also performed using MATLAB.

Quantifying neuronal activity

We looked for visual responses in the time period 25–200 ms after target onset. To determine the beginning of the time window to be used for calculating mean visual responses for each neuron, we first calculated a visual response histogram over all trials for all targets. We then fit a normal cumulative distribution function to the response histogram from 25 ms after target onset until the peak of the response. We took the start of our time window to be the time at which the fit curve reached half height. To determine the end of the time window used to calculate mean visual responses, we fit the mean response histogram to a Weibull probability density function. The end of the visual response time window was taken as the time that the fit curve decreased to half height after the peak (McAlonan et al., 2008). Note that the end of the response time window could not exceed 200 ms (the end of the epoch being considered), nor could this visual time window be shorter than 20 ms.

Response time windows used to calculate saccadic activity were determined in a nearly identical manner. We again fit a normal cumulative distribution function to determine the beginning of the window and a Weibull probability density function to determine the end of the window, the only difference from visual responses being that we looked for saccadic activity from 150 ms before saccade onset until 150 ms after saccade onset, and only for correct saccades.

Once we had determined the visual response time window and the saccadic activity window for each neuron, mean neuronal responses were calculated within these windows for each target position. For each neuron, we used a single time window for all target locations because we would have been unable to calculate individual time windows for target locations that had no visual or saccadic activity: the fit curves would be flat.

Neuronal activity latencies

The latencies of visual responses and saccadic activities were derived from the same normal cumulative fits above used to determine the beginning of the response windows. We took the latency of the activity to be the time of the fit curve's rise to 10% of its peak (rather than using the 50% mark as for the time window). We did this for both visual responses and saccadic activity. Determining activity latencies in this manner provides latency estimates that correspond well to the observed response histograms, works well for both fast and slow responses, and provides latencies that are directly comparable with other work in our lab (McAlonan et al., 2008).

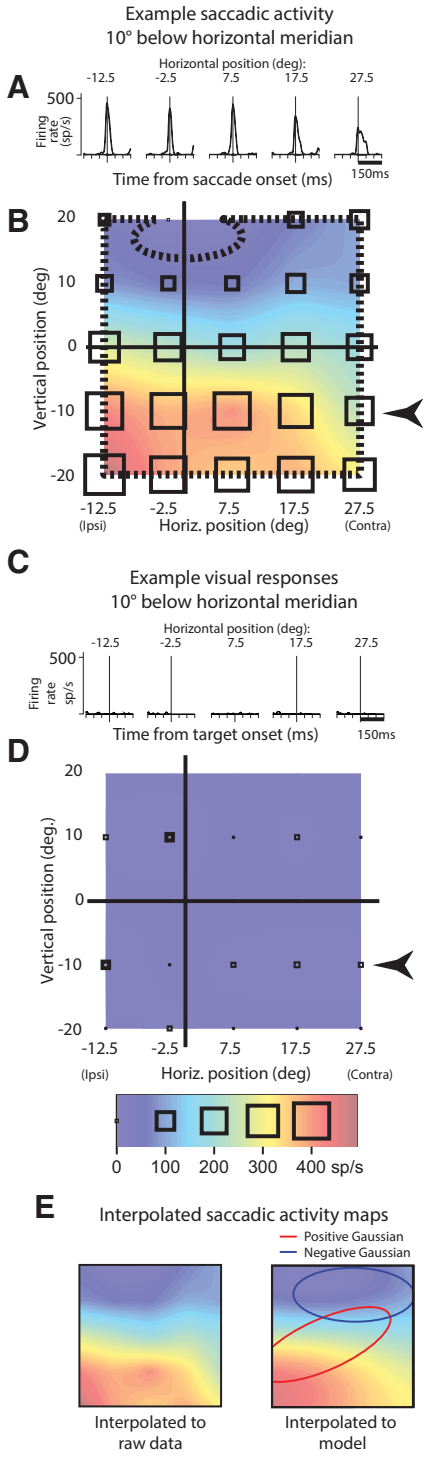

Figure 1. Example presaccadic neuron with a bilateral visual field. ***A***, Spike density plots for saccades to all five targets in a horizontal row 10° below the horizontal meridian (black arrow at the right side of panel ***B*** indicates the row of targets for which responses are plotted). Curves were smoothed with a 5-ms SD. Gaussian filter. Presaccadic activity was strong in both the ipsilateral and contralateral visual field. ***B***, Visual field map of saccadic activity for the same neuron. Horizontal and vertical meridians are represented by the black lines. The area of each open square is proportional to the neuronal response for a stimulus located at the center of each square. The background color indicates the interpolated gradient of activity. The scale for the squares and the calibration of the colored background is at the bottom of the figure. The thick black dashed line enclosing the field represents the region of the visual field (according to the Gaussian fits, see Materials and Methods), where all responses were above 3 SDs of the background. The black arrow to the right of the grid indicates the row of targets for which the saccadic activity is plotted in panel A. The presaccadic activity was clear in the ipsilateral visual field as well as in the contralateral visual field. ***C***, ***D***, Visual responses to saccade targets, in the same format as in ***A***, ***B***. Responses are aligned to target onset. For this neuron, visual responses were minimal in both the ipsilateral and contralateral visual fields. ***E***, Comparison of raw and fit interpolated saccadic activity maps. The left panel shows the activity map interpolated to the raw data from panel ***B***. The raw data were fit to two Gaussians (one positive and one negative) as described in Materials and Methods. The right panel shows the two Gaussians (red: positive, blue: negative) and the resulting activity map. Activity maps from the fits provided less noisy estimates of field size and shape.

Activity maps

Spatial patterns of visual responses and saccadic activities for each neuron were visualized by creating two-dimensional matrices of neuronal activity, plotting the activity at each target location. We created one matrix for visual responses and one for saccadic activities. These response matrices allowed us to calculate initial response characteristics.

First, we determined the existence of either a visual receptive field or a saccadic movement field. For a field to exist, the response matrices had to pass two criteria. The first was subjective; we looked at the response matrix and decided whether or not we could see a pattern of activity consistent with a field, rather than just random variations across the visual field. Second, we developed a quantitative procedure that reflected our subjective decisions and used the same procedure for both visual and saccadic fields. We first normalized each response in the grid by the SD of the baseline activity. Any responses below 1 SD of baseline activity were set to zero. We called this normalized response Rsp_{SD}. We then calculated the average Rsp_{SD} over all grid locations. Comparing Rsp_{SD} to our qualitative assessments, we decided that visual responses formed a visual receptive field if the average visual Rsp_{SD} (over all target locations) was >1.0. A saccadic movement field was said to be present if the average saccadic Rsp_{SD} was >2.0. This method recognized small fields with strong responses as well as large fields with less robust responses. We used different criteria for visual and saccadic fields (1.0 vs 2.0, respectively) because in lateral MD, visual responses were much less prominent than saccadic activity, and we wanted to include more visual activity for comparison with saccadic movement fields. Note that this also overestimated the number of visual receptive fields we recognized. Response matrices had to pass both criteria to show the existence of a visual or saccadic field.

Next, we determined a saccadic index for each neuron, indicating whether the neuron's strongest activity was saccadic or visual. This index used only the maximum mean saccadic activity from the entire response matrix (S_{max}), and the maximum visual activity (V_{max}). The saccadic index was simply: $(S_{max} - V_{max})/(S_{max} + V_{max})$. Neurons with purely saccadic activity would have a saccadic index of 1.0, and neurons with only visual responses would have a saccadic index of -1.0.

We next determined the degree to which neuronal activity (visual and saccadic) occurred in the visual hemifield ipsilateral to the neuronal recording site. To do this, we only considered target locations with significant responses. Individual responses in the response matrix that exceeded baseline activity by three SD of the baseline firing rate were considered to be significant. As we initially expected most neuronal activity to be contralateral to the recording site in MD, we centered our stimulus grid toward the contralateral side of fixation, which meant recording from more contralateral targets than ipsilateral targets in a given experiment. To compare the activity between the contralateral and ipsilateral hemifields, we considered responses for targets in the contralateral and ipsilateral visual fields the same distance from the vertical meridian. We added all the significant responses in the contralateral hemifield (R_c) and in the ipsilateral hemifield (R_i). To demonstrate laterality of neuronal activity, our contralateral index was, therefore, $(R_c - R_i)/(R_c + R_i)$.

Neurons with responses only in the contralateral hemifield would have an index of 1.0, whereas purely ipsilateral neuronal activity yielded an index of -1.0.

Field size and shape

Once we determined the existence of either a visual receptive field or a saccadic movement field as above, we then quantitatively determined the

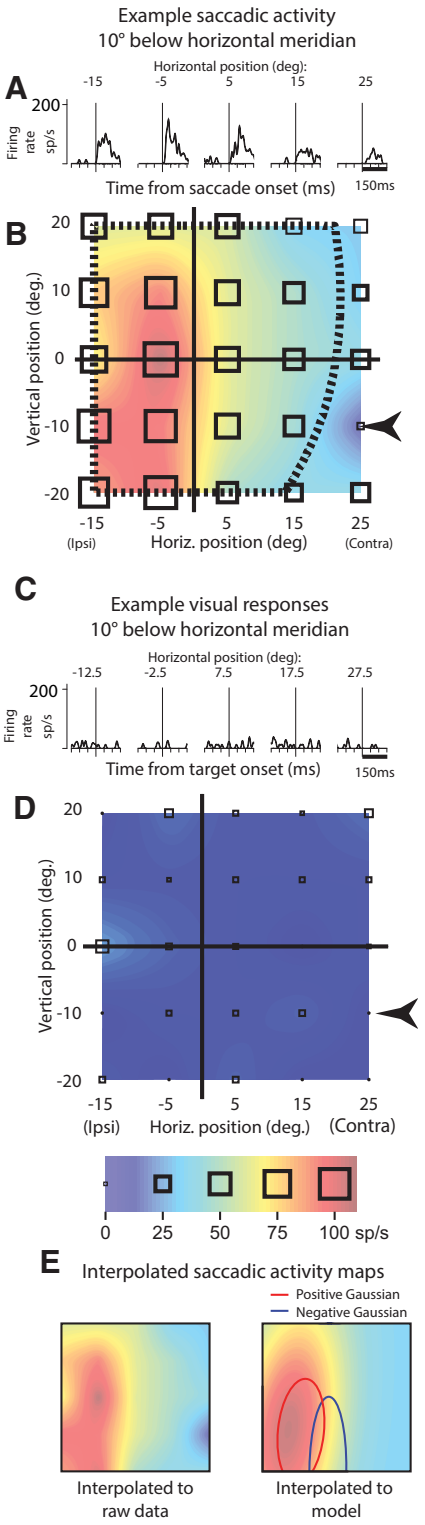

Figure 2. An example neuron with postsaccadic activity in both the ipsilateral and contralateral visual fields. The same organization as in Figure 1 but with slightly different horizontal target placement. ***A***, ***B***, Example of the postsaccadic activity of the neuron for targets 10° below the horizontal meridian, and the saccadic activity map (calibrations again at the bottom of the figure). Postsaccadic activity was strongest for this neuron in the ipsilateral visual field. ***C***, ***D***, Visual responses and visual field map showing little response to the saccade target. ***E***, Comparison of raw and fit interpolated saccadic activity maps. The left panel shows the activity map interpolated to the raw data from panel ***B***. Symbol meanings as in Figure 1*E*.

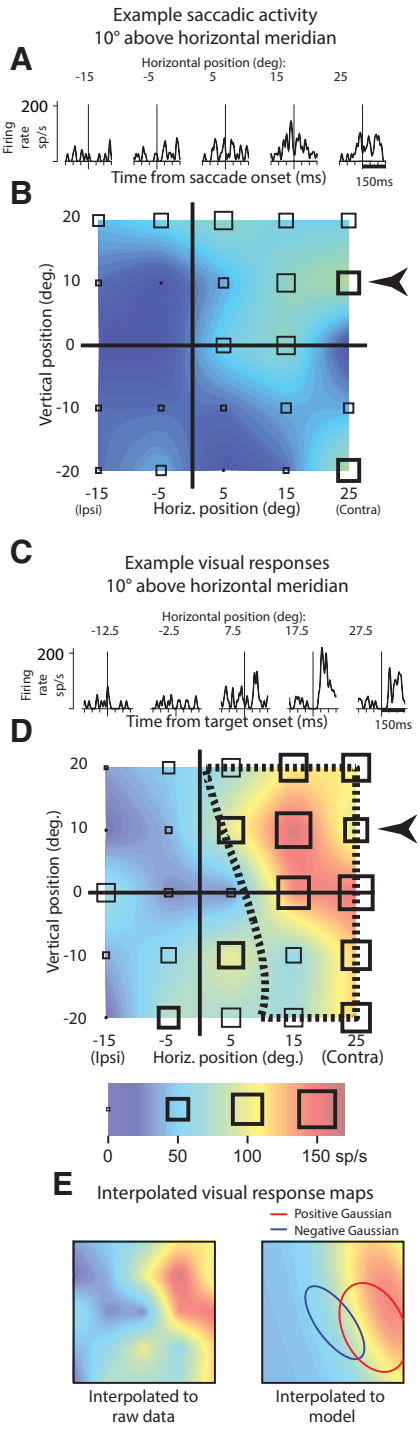

Figure 3. An example neuron with predominantly visual activity. Same organization, symbols, and keys as in Figures 1, 2. ***A***, ***B***, Saccadic activity showing significant activity only for saccades to two contralateral stimuli. ***C***, ***D***, Significant visual responses almost exclusively in the contralateral visual field. ***E***, Comparison of raw and fit interpolated visual response maps. The left panel shows the activity map interpolated to the raw data from panel ***D***. Symbol meanings as in Figure 2*E*.

size and shape of these fields. Our first step was to interpolate the response matrix at 0.1° resolution using MATLAB's (MathWorks) TriScatteredInterp function with natural neighbor interpolation. Using a high resolution for the interpolated map yielded much smoother contours for field size and field shape. We then fit a difference of two-dimensional Gaussians to the interpolated surface. Each Gaussian was allowed to adjust its center, X-SD and Y-SD, and orientation to best fit

the surface. The resulting fit surfaces matched the data well overall, but this fit was purely descriptive, so we placed no importance on the actual Gaussians produced by the fit. Both field extent and field shape were calculated from the fit surface.

For field size, we first determined the area of the fit surface that exceeded three SD of the baseline response (the same criterion used for significant responses in the response matrix). We then converted this area measurement into an equivalent diameter:

$$D = 2\sqrt{\frac{A}{\pi}},$$

which is the diameter D of a circle with an area A equal to that of the field. This measurement was used to compare field sizes.

To quantify field shape, we focused on one particular spatial aspect of two-dimensional shapes: concavity. The greater the concavity, the greater the field irregularity, whereas fields with no concavities would be considered regular. Field regularity was therefore represented as the inverse of the degree of concavity of the field profile. We used the same surface fit to the data as above for field size, but this time, we calculated the contour of this surface that exceeded half of its maximum value (half-height contour). This yielded representations of field shape that were independent of overall response strength, as many large fields with significant responses throughout still exhibited clearly irregular spatial structure. We then calculated the convex hull of this half-height contour. Field regularity was simply the ratio of the area of the convex hull to the area of the half-height contour.

Grid-aligned MRI localization of recording sites

To establish the anatomic locations of recording sites in lateral MD, we used the same technique as in Cavanaugh et al. (2016), which capitalized on visualization of the grid and chamber geometry in structural MRI images. We used a custom application described previously (Cavanaugh et al., 2016), implemented as a plug-in for ImageJ (Schneider et al., 2012). First, we rotated the 3D MRI dataset in three dimensions so that the rotated MRI volume was aligned to the grid (visible in the MRI). Second, we selected the boundaries of the grid and, with the custom plug-in, zeroed the MRI image coordinate frame to the center of the grid. We entered the anterior/posterior (AP) and medial/lateral (ML) grid coordinates (in millimeters), and the depth of each of each recording (in micrometers). The plug-in then calculated the *x*-, *y*-, and *z*-coordinates of each recording site within the MRI and placed a mark on the appropriate MRI slice. Lesions were made by passing current (12 μA for 6 min) through an Elgiloy electrode (Koyano et al., 2011), and we had verified the alignment of the visible lesions with their marked locations in the previous study (Cavanaugh et al., 2016).

In the MRI, we only determined the locations of neurons that discharged before or after saccades or had visual responses to the saccade target. An advantage of registering recording locations using the MRI is that the MRI does not shrink, unlike histologically prepared tissue. A disadvantage is that the exact anatomic location was less precise than it would have been with histology. We then converted our MRI locations onto a standard macaque monkey atlas available on the web (Dubach and Bowden, 2009; Rohlfing et al., 2012) to facilitate the use of our localizations for future experiments in lateral MD. This conversion was done in two stages.

We first aligned MRI slices to coronal sections from the monkey brain atlas. For aligning along the AP dimension, our key landmarks were the anterior and posterior commissures, as our focus was the thalamus. We located both the MRI section and the atlas section closest to the AP center of the anterior commissure (AC), and again for the posterior commissure. We then matched up MRI slices with atlas sections by their relative distance between these two landmarks. For example, the MRI slice 30% of the way from the posterior commissure to the AC would correspond to the atlas slice 30% of the way from the posterior commissure to the AC. Because of the different AP resolutions of the MRI and the atlas, the corresponding AP locations were not always exact but never differed by >0.45 mm.

We then aligned each MRI slice to its corresponding atlas section using unmistakable landmarks. For horizontal alignment, we used the brain midline. For vertical alignment, we used the clearly visible lateral ventricles and corpus callosum. This entire alignment procedure allowed us to plot the locations of our recordings on an established online macaque brain atlas and to confirm that our recording locations were where we expected them to be.

Finally, we converted the atlas AC coordinates (Paxinos et al., 2000; distance from the AC along an axis through the anterior and posterior commissures) to Horsley–Clarke coordinates (distance from the external auditory meatus along the meatal/orbital axis). As the two coordinate systems are based on different landmarks, the Horsley–Clarke meatal/orbital axis tilted slightly downward in the rostral direction relative to the commissural axis. The tilt is less than a degree and made a negligible difference in the short AP distance we considered, so we did not compensate for it.

We refer to the neurons studied as saccade-related CD neurons because they have the same saccade-related activity as those previously shown to receive input from SC and project to FEF (Sommer and Wurtz, 2004a). In addition, these neurons are in the same area as those that were inactivated to produce CD-dependent changes in saccades (Sommer and Wurtz, 2002, 2004b) and in perception of eye location (Cavanaugh et al., 2016). We cannot exclude the possibility that other saccade-related neurons that are not CD neurons are also included, as pointed out in Discussion.

Results

We determined the saccadic and visual activity as the monkey made saccades to targets in the contralateral and ipsilateral visual fields. Systematic electrode penetrations were made through the lateral areas of MD thalamus in one hemisphere of monkey O and two hemispheres of monkey C. We concentrated on the lateral regions of MD where previous experiments found the highest prevalence of saccade-related CD activity (Sommer and Wurtz, 2004a). We concentrated on neurons that could be clearly isolated. The CD-related neurons are clearly imbedded in lateral MD among other neurons that do not have the characteristics of CD related neurons. At this point there is no reason to assume that these other neurons are either related to a CD or are completely independent of a CD function. We concentrated on recording from CD related neurons to record as many neurons in a session as possible and to test as many neurons on a penetration as possible.

Movement fields and visual receptive fields of lateral MD neurons

We recorded from 141 neurons in lateral MD with saccadic and/or visual activity (39 from monkey O, 102 from monkey C). Of these 141 neurons, only about half of them had consistent responses over the visual field that yielded either visual response maps or saccadic activity maps (24 from O and 47 from C, 71 total). We acquired these saccadic and visual maps while the monkey made saccades to targets within a 5×5 grid with 10° separation between locations. As our stimulus locations were separated by 10°, it is possible that we might have overlooked some smaller movement fields closer to the fovea. We do not think this affected our overall results as the visual and/or saccadic activity was first assessed manually and the stimuli were placed accordingly. Moreover, although saccadic movement fields were often large, we were successful in measuring many smaller fields (down to 4° diameter) closer to the fovea: enough to calculate a significant correlation between field diameter and field eccentricity ($r = 0.46$, $p = 0.0002$).

Our target grid encroached on the ipsilateral visual field, but most targets remained in the contralateral hemifield. We anticipated that a greater representation of the contralateral field would enable us to verify that our neurons were like those studied previously (Sommer and Wurtz, 2004a) and would allow us to get a more accurate estimate of movement field size. Because of the size of the movement fields, however, the full extent of most movement fields could not be determined by our target grid.

For saccadic neurons in both monkeys, we found some that increased their discharge before the saccade (presaccadic) and some after the saccade (postsaccadic). Figure 1 shows an example neuron with activity beginning before saccades to targets in the ipsilateral and contralateral visual fields. Figure 1*A* shows activity for saccades to the row of targets 10° below the horizontal meridian, where saccadic activity was greatest. This row of targets is indicated on the activity map by a black arrow to the right of Figure 1*B*. The averaged neuronal activity in the histograms is aligned on saccade onset. This neuron showed equally vigorous activity in the ipsilateral and contralateral visual fields.

The 5 × 5 matrix of responses to the targets on the grid (Fig. 1*B*) shows that robust neuronal activity preceded saccades to targets in both the ipsilateral and contralateral visual fields. The area of the square boxes centered on each target location indicates the magnitude of the activity for a saccade to that target, and the colored background shows the interpolated magnitude of the activity between these data points. The arrow to the right of the panel indicates the row of targets for which example response histograms are shown above the response matrix. Note that this neuron exhibited strong activity before saccades to targets in both visual hemifields. Figure 1*C*,*D* shows the lack of visual responses to the same targets in either visual hemifield. Figure 1*E* demonstrates how the interpolated saccadic activity map is refined by the descriptive fit described in Materials and Methods.

Figure 2 shows an even more striking example of a neuron with ipsilateral saccadic activity (Fig. 2*A*). In this case, the response histograms show the neuron had postsaccadic rather than presaccadic activity, but the saccadic activity was stronger in the ipsilateral visual hemifield. Again, this neuron had very little visual response (Fig. 2*C*,*D*). MD neurons clearly were active for saccades to ipsilateral as well as contralateral targets. It is unlikely that visual stimulation during the saccade contributed to the postsaccadic activity because the majority of these neurons had little visual response.

Some neurons, however (Fig. 3 shows an example), did have some saccade-related activity (Fig. 3*A*,*B*) as well as stronger visual responses (Fig. 3*C*,*D*). In this example, both the presaccadic activity and the visual responses were centered in the contralateral visual field.

Figure 4 shows the distributions of the characteristics exemplified in Figures 1–3 across our sample of 71 neurons for which we found either saccadic or visual fields. Figure 4*A* shows a scatterplot of the 71 neurons with saccadic and/or visual field maps showing both the maximum saccadic and visual activities for each neuron. The value plotted for each neuron is the maximum value from the response grid. Note that maximum values for neurons with especially variable activity may appear spuriously high (e.g., the open symbols showing high maximum saccadic activity for neurons without a saccadic map). Most cells lie below the unity diagonal indicating that neuronal activity in lateral MD neurons is predominantly saccadic. Only those neurons with presaccadic activity (red points) should be considered as CD neurons. The saccade-related neurons were predominantly presaccadic.

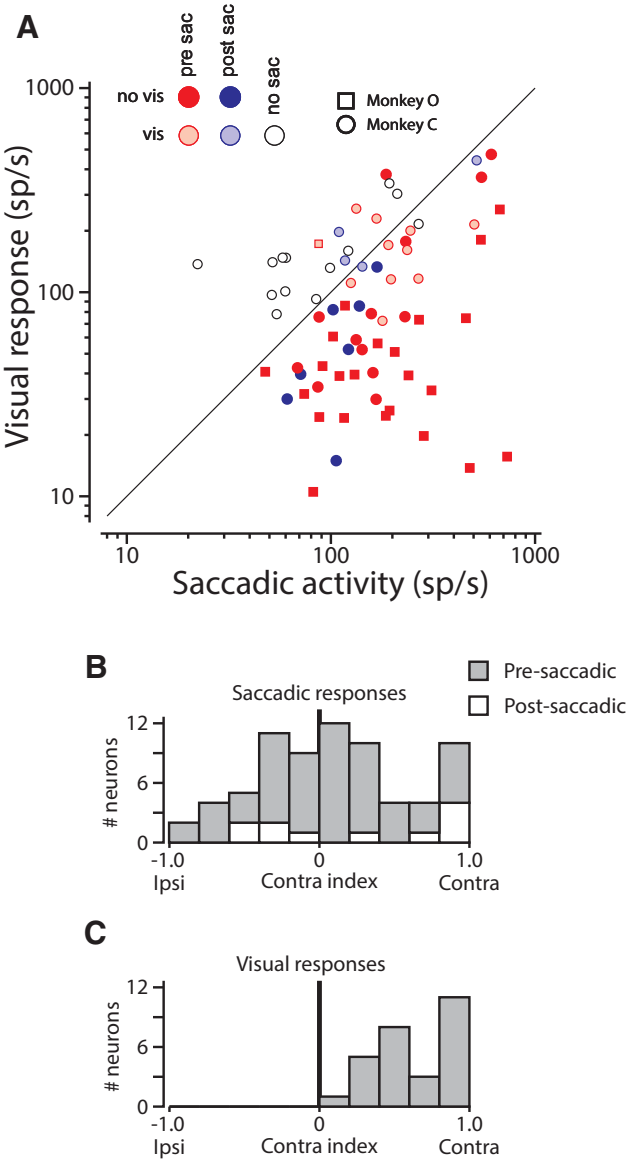

Figure 4. Comparison of saccadic and visual activity across the sample of neurons. ***A***, Scatterplot of maximum saccadic and visual activity for 71 neurons with presaccadic (47), postsaccadic (11), and no saccadic activity (13), and with or without visual responses. Neurons from monkey C are plotted as circles, and neurons from monkey O are plotted as squares. ***B***, Contralateral indices of saccadic activity for both monkeys. Apart from a number of neurons with saccadic maps that were exclusively contralateral (index of 1.0), saccadic neurons had movement fields distributed similarly between ipsilateral and contralateral visual hemifields. ***C***, Contralateral Indices for visual activity for both monkeys. Indices for visual responses are exclusively greater than zero, meaning that although visual activity did sometimes spread into the ipsilateral visual hemifield (index < 1.0), no neuron's visual responses were predominantly ipsilateral.

Over our population of saccade-related neurons, presaccadic activity ranged from 87 to 518 spikes/s, averaging 215 spikes/s (SD = 131 spikes/s). The baseline firing rate (before target presentation) was 44 spikes/s (SD = 35 spikes/s).

Figure 4*B*,*C* shows the distributions of activity in the contralateral and ipsilateral visual fields for saccadic activity and visual responses, respectively. We quantified the degree to which neuronal activity was confined to the contralateral visual field with a contralateral index (see Materials and Methods), which was 1 if all activity was in the contralateral field, −1 if all activity was in the ipsilateral field, and 0 if the activity was evenly distributed across the vertical meridian.

Across our sample, saccadic activity was distributed through both the ipsilateral and contralateral hemifields, with activity interestingly represented more strongly in the ipsilateral hemifield for many neurons. Still, the net bias for saccadic activity was in the contralateral hemifield (mean contralateral index = 0.42 ± 0.48 SD, $p = 0.0099$, signed-rank test). In contrast, visual activity (Fig. 4*C*) was exclusively centered in the contralateral visual field, with no contralateral index falling below 0.20 (mean contralateral index = 0.67 ± 0.31 SD, $p < 10^{-5}$, signed-rank test). The neurons with presaccadic activity are all candidates for carrying the CD signal, but of course, this is an inference from previous studies showing that neurons in this area did not drive saccades (Sommer and Wurtz, 2004b, 2008). We do not speculate on function of the postsaccadic neurons.

We computed a similar index characterizing the distribution of neuronal activity between the upper and lower visual fields. Within our population of saccadic neurons, there was no difference in the frequency of activity between the upper and lower visual hemifields (mean index = 0.065 ± 0.46 SD, $p = 0.89$, signed-rank test) although many neurons did prefer either the upper or lower hemifields.

In summary, many saccade-related neurons showed vigorous activity with saccades directed into the ipsilateral visual field as well as the contralateral field. In contrast, visual responses were centered in the contralateral visual field. Although movement fields and visual fields often were often not mapped in their entirety, movement fields were typically large, frequently approaching nearly a full quadrant of the visual field. Furthermore, from the example fields shown in Figures 1–3, the fields were frequently large enough to include both the foveal region around the fixation point and the peripheral visual field.

Spatial regularity of movement and visual receptive field profiles

The saccadic movement fields shown so far (Figs. 1*B*, 2*B*) had reasonably regular spatial organization not inconsistent with a two-dimensional Gaussian profile; activity systematically decreased with distance from the movement field center. There were, however, many striking exceptions that must be noted. Figure 5 shows two saccadic activity maps that had remarkably irregular spatial patterns. In Figure 5*A*, the saccadic activity is in the upper and lower contralateral visual field with a region of low saccadic activity along the horizontal meridian. In Figure 5*B*, a similar region of low activity is present but in the upper ipsilateral visual field. We calculated a regularity index to quantify such bifurcations of saccadic and visual fields using the ratio between the field's actual area, and its area assuming no concavities (see Materials and Methods). A regularity index of 1 indicates a completely convex field. Figure 5*C* shows a substantial number of irregular saccadic movement fields (regularity index < 1), but Figure 5*D* shows far fewer irregular visual receptive fields. We do not know whether these irregular fields represent an inadequacy in our methods to fully reveal the true shape of these fields, or whether these irregularities have significance for the underlying neuronal mechanisms. In any case, these spatial irregularities, although not a universal characteristic of all the fields we measured, were frequent enough to note their occurrence.

Anatomical location of CD neurons within a lateral thalamic band in MD

Future experiments on the relay neurons that convey CD signals. As explained in detail in Materials and Methods, the locations of the saccade-related neurons were plotted on a series of standard

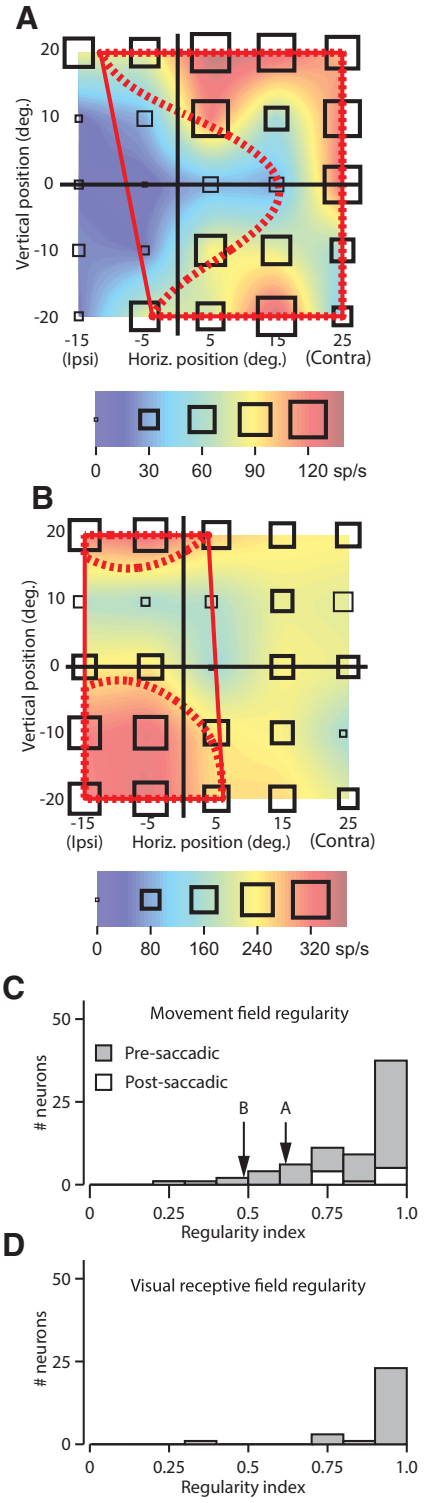

Figure 5. Irregularity of saccadic movement fields. ***A***, Saccadic activity predominantly in the contralateral field of an example neuron with a pocket of no activity along the vertical median. The thick red dashed line shows the contour of the movement field at 50% of the maximum response. The solid red line shows the minimum convex region enclosing the movement field contour. ***B***, Saccade-related activity of another neuron with a sparse activity in the central visual field, but with the strongest saccadic activity in the ipsilateral visual field. ***C***, Distribution of irregularity indices (see Materials and Methods, Field size and shape) for saccadic movement fields. Arrows indicate the values for the neurons in ***A***, ***B***. ***D***, Distribution of irregularity indices for visual receptive fields. With only few exceptions, visual receptive fields were essentially regular in shape. Saccadic movement fields were significantly more irregular than visual fields ($p = 0.0002$, rank sum).

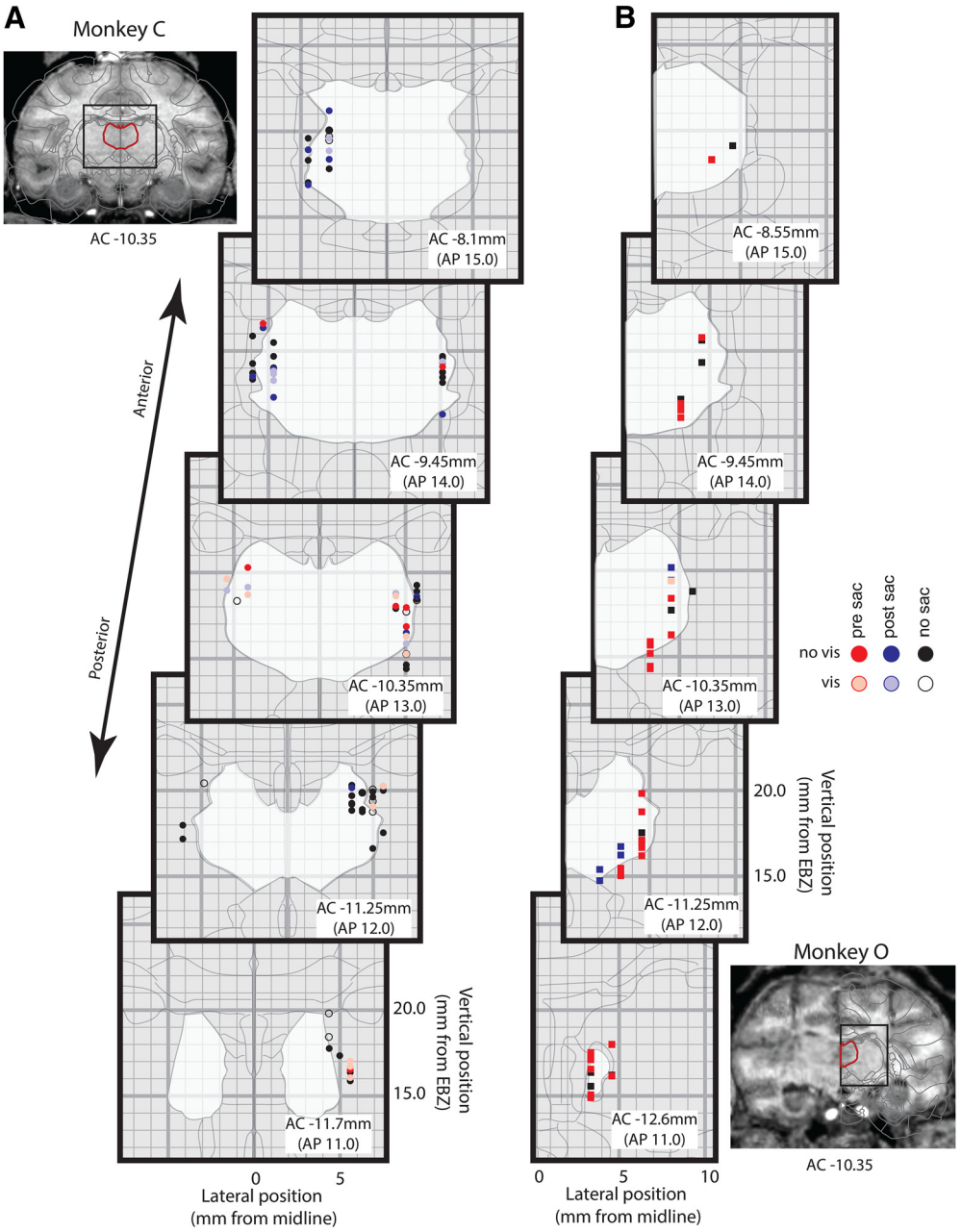

Figure 6. Anatomical reconstruction of recording sites. ***A***, Location of neurons in monkey C. Symbols are circles for monkey C. The top left panel shows an entire MRI coronal section from AC −10.35 mm. The region of interest in the thalamus, MD, is outlined in red, and the black rectangle shows the region reproduced in the adjacent column of atlas sections. The adjacent column of panels shows recording locations superimposed on schematic coronal representations of MD thalamus (white area) at a series anterior-posterior locations. Gray contours within the rectangles show anatomic boundaries derived from the reference atlas (see Materials and Methods). The AC coordinates are shown for each section with the corresponding Horsley–Clarke AP coordinates in parentheses. Neurons cluster at the lateral edge of MD. ***B***, Location of recording sites in monkey O. Symbols are square for monkey O. The bottom right panel shows the entire MRI coronal section at the same anterior-posterior location as in ***A*** (AC −10.35 mm). We recorded from only one hemisphere in monkey O. Again, our neurons cluster at the lateral edge of MD.

atlas coronal sections by aligning the anterior and posterior commissures in the MRI and the atlas. Figure 6 shows the location of all 141 neurons from which we recorded (A Monkey C, B Monkey O). The brain areas containing saccadic or visual neurons are shown on the coronal sections of monkey C (left column, both hemispheres) and monkey O (right column, left hemisphere). MD is indicated by the white central area. The legend indicates which neurons had saccadic activity, visual responses, or both. The 70 neurons with neither visual nor saccadic fields are shown as black dots. (Note that the discrete grid-based locations of our penetrations, coupled with the limited depths over which the neurons were found in MD, result in a substantial overlap of symbols for neurons with similar characteristics; not all locations may be visible because of overlap, but they have all been plotted.) We made many more penetrations outside of the MD region reported. These penetrations yielded neither visual nor saccadic activity, and are therefore not shown.

We found saccadic and visual activity in lateral MD neurons ranging from Horsley–Clarke AP11 to AP15: a distance of ~4–5 mm. The lateral distance from midline to saccadic and visual neurons understandably varied among sections but followed the lateral edge of MD as reported previously for CD relay neurons.

Our digital anatomic reconstruction provides a better determination of the location of the neurons carrying CD signals in MD thalamus, as we were able to plot the locations of these neurons in three dimensions relative to both the anatomic MRI, and an established brain atlas.

Although our grid-based volumetric algorithm located the great majority of neurons in lateral MD as defined by the atlas, a few were located more laterally or dorsally, most likely because of the fact that every brain does not exactly match the atlas. Unfortunately, we cannot rule out the possibility that some saccade-related neurons were in fact located past the lateral edge of MD, but given the accumulated spatial uncertainties in registering penetration data from both the MRI and the atlas, we think it likely that the saccade-related neurons we recorded were all within lateral MD.

Figure 7 shows a summary for the location of just the presaccadic neurons, which are the only neurons that could be carrying a CD signal. Because the three hemispheres shown in Figure 6 were all plotted on the same standard atlas sections, which are symmetrical for the two sides of the brain, we combined them by simply superimposing the three hemispheres. The combined map confirms that saccade-related neurons clustered in a band at the lateral edge of MD. Although we do not have histologic verification of the exact region of the thalamus in which these neurons cluster, there is little doubt from their lateral position that they fall into the parvocelular division of MD rather than the more medial and anterior magnocelluar division (Jones, 2007; pp 1177–1180).

Functional organization of saccadic and visual neurons in the MD lateral band

The grid of electrode penetrations in MD allowed us to evaluate whether there was any spatial organization of neuronal response properties within the CD neurons in MD. One prominent characteristic of all saccadic neurons in lateral MD was their typically large movement fields (median 21.7° equivalent diameter, 13.0° median absolute deviation) and similarly large visual receptive fields (median 16.3° equivalent diameter, 9.0° median absolute deviation). We saw no indication of any systematic organization of movement or visual field centers within the volume of the lateral band, although our estimates of field centers were limited by our inability to determine the peripheral edges of the large fields. Given the size of these visual receptive fields and saccadic movement fields, it is not surprising that we saw no retinotopic organization, just as was reported previously (Sommer and Wurtz, 2004a).

We did, however, find two consistent relationships between response characteristics and neuronal location within lateral MD (Fig. 8). Figure 8*A* shows how neuronal activity became less related to visual stimuli and more saccade-related as neuronal depth increased. Saccade-related neurons were consistently deeper. Note, however, that the data for visual activity are predominantly in one monkey. As we focused on saccadic CD neurons in the second monkey, we did not seek to record from the shallower visual neurons but instead used them as the harbingers of the deeper saccadic neurons. Thus, although not documented, this trend held for the second monkey as well.

Figure 8*B* plots the onset of saccadic activity against anterior-posterior location within lateral MD. Neurons with postsaccadic activity began appearing as we moved more anterior within lateral MD, although the presaccadic neurons persisted anteriorly. For other characteristics of the MD neurons, we found little or no relation to anatomic position in the lateral band.

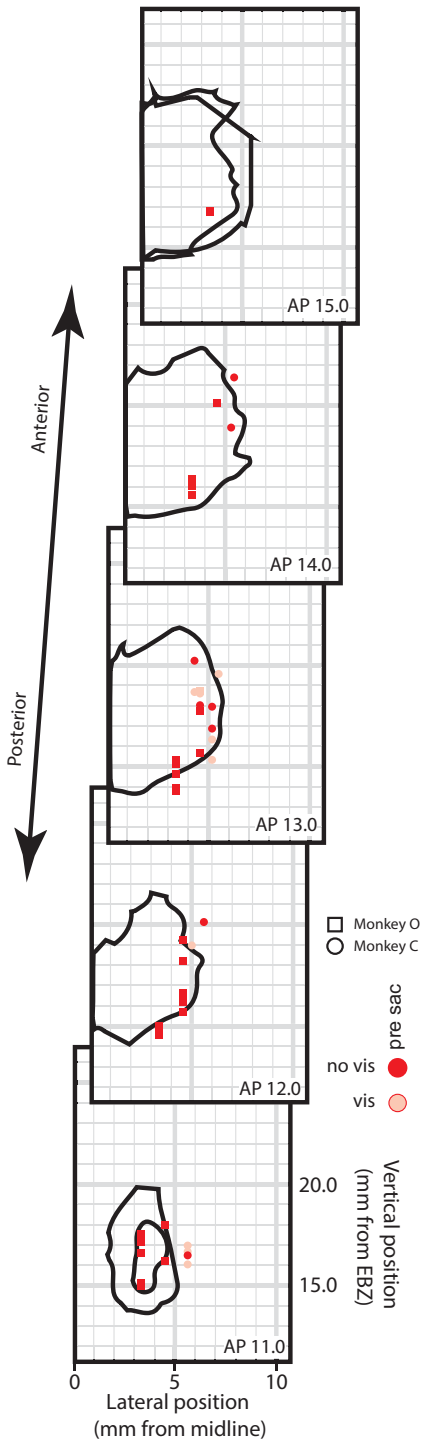

Figure 7. Summary of all neurons with presaccadic activity in lateral MD. Circles are presaccadic neurons from monkey C, and squares are presaccadic neurons from monkey O. The locations of the 47 neurons from the three hemispheres in two monkeys shown in Figure 6 are plotted on the same AP sections. Horsley–Clarke coordinates are shown in each section.

In summary, locating the band of saccade-related CD neurons in lateral MD should be facilitated by two key results of the present experiments. First, based on the grid of penetrations through lateral MD, the anterior-posterior and medial-lateral location of the CD neurons now have more exact specifications in stereotaxic coordinates. Second, using the observation that the saccade-related CD neurons are just below neurons with visual responses provides an online marker for locating the depth of the CD neurons.

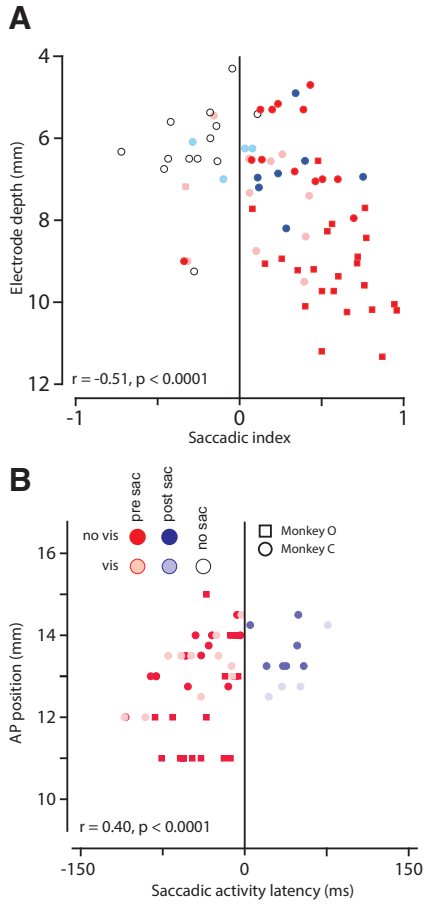

Figure 8. Two correlations between neuronal characteristics and anatomic location within the lateral band. ***A***, Scatterplot showing relationship of saccadic index to depth in MD. Neurons deeper in MD tended to favor saccadic activity over visual responses. Purely visual neurons were found only at shallower depths. Symbol shape again denotes monkey. ***B***, Scatterplot showing relationship of saccadic activity latency to Horsley–Clarke anterior-posterior position in MD. As we recorded neurons more anterior in MD, saccadic activity latency increased. That is, more neurons with postsaccadic activity were found the more anteriorly we went in MD.

Discussion

We addressed two salient questions related to the MD thalamus relay neurons in the established CD circuit from SC to FEF, recording from a grid of locations in lateral MD. First, although previous studies of the CD neurons showed activity consistent with contralateral visual field representation, we found that CD neurons were also active before saccades to ipsilateral targets. The bilaterality of saccadic activity in cortex is already established in the thalamus. Second, we found the saccade-related neurons to be concentrated in a clear band along the lateral border of MD.

Bilateral movement fields for saccade-related CD neurons

In FEF, increased neuronal activity precedes saccades to target locations both contralateral and ipsilateral to the FEF being studied. Crapse and Sommer (2009) have shown that this bilaterality results from inputs from both sides of the SC. Furthermore, in hemi-decorticated humans, saccade-related CD is still available in the remaining hemisphere for bilateral saccades (Rath-Wilson and Guitton, 2015). Our experiments raise the possibility that a major source of this bilateral information is MD thalamus. By plotting the movement fields for MD neurons with saccade-related activity, we showed that most neurons are active for saccades to both ipsilateral and contralateral visual fields. While we could not measure the full extent of most MD movement fields, they extended similarly into the ipsilateral and contralateral visual fields. This is consistent with the recent finding that muscimol inactivation of lateral MD impairs a monkey's ability to perceive the ending location of its eye movements after saccades made into both visual fields (Cavanaugh et al., 2016).

For the FEF, Crapse and Sommer (2009) showed conclusively that many neurons have input from the SC ipsilateral to the FEF (for saccades into the contralateral visual field) but also from the SC contralateral to the FEF (for saccades into the ipsilateral field). At the start of the pathway in SC, the strongest presaccadic activity is before saccades toward the contralateral visual field, with only neurons nearly on the vertical meridian active before ipsilateral saccades (Wurtz and Goldberg, 1972; Wurtz and Albano, 1980; Sparks, 1986) and with foveal presaccadic activity limited to contralateral saccades (Chen et al., 2019). From the current study, the bilaterality of the MD neurons shows that the crossing of saccadic activity must occur in or before MD thalamus but after SC.

Where the crossover point is located has not been determined. One possibility is that it occurs in the massa intermedia of the thalamus as suggested by Crapse and Sommer (2009). Input from the SC crossing before synapsing on MD neurons would be consistent with our current observations. Thus, while the neurons in MD do not have projections crossing the midline in the massa intermedia, just as is the case in the dorsal thalamus in general (Jones, 2007), bilaterality is produced by a crossing of inputs from the SC. This also suggests that the crossed SC input to MD arises largely from the SC saccade-related neurons that do not have visual responses because we find that MD neurons with ipsilateral movement fields do not have ipsilateral visual receptive fields.

Of course, one alternative to the crossing in the massa intermedia would be a crossover that occurs in the collicular commissure rather than in the massa intermedia. Two other possibilities also must be mentioned. One is that the presaccadic activity in the SC includes some activity before ipsilateral saccades, but any evidence for this is slight (Mohler and Wurtz, 1976; Sparks, 1986; Chen et al., 2019). Another possibility is that the source of ipsilateral visual field activity with saccades is a result of input from cortico-thalamic crossed projections to lateral MD (Kunzle, 1976; Preuss and Goldman-Rakic, 1987), but this is unlikely because although activity of FEF neurons is bilateral, bilateral visual activity in MD is not strong.

What saccade-related CD neurons tell Us about MD thalamus

The characteristics of MD saccade-related neurons indicate that MD is not a passive relay, much as the lateral geniculate nucleus (LGN) is not a passive relay. The MD neurons would be best described as combining saccade-related information rather than just relaying it. The most striking case of course is the profound bilaterality of saccadic activity in lateral MD that is absent in the SC input. This bilaterality conveyed to FEF might well be conveyed to other areas of frontal cortex as indicated by the wide anatomic projections of MD (Goldman-Rakic and Porrino, 1985; Erickson and Lewis, 2004). A second piece of evidence is the consistently larger size of MD saccadic movement fields compared with those in SC. In SC, movement fields become larger as their eccentricity increases (Wurtz and Goldberg, 1972; Mohler and Wurtz, 1976; Sparks, 1986). We found a similar correlation

between field size and eccentricity in MD, indicating common representations. But the larger movement fields in MD suggest a combining of inputs from across wider but similar areas of the SC map. The net point is that the MD neurons combine information rather than simply pass on their SC input to frontal cortex. Access to information from both ipsilateral and contralateral visual fields and from much larger movement fields provides a CD in MD that covers a much larger area of the visual field than does the CD in SC. What the benefit of this expansion is remains to be determined.

Location of saccade-related neurons in MD

Our second contribution is the more exact location of the saccade-related neurons in a lateral band in MD. A number of previous studies have identified saccade-related neurons in the thalamus and, while most are clearly out of the lateral band we have identified, some could be in overlapping areas. Schlag-Rey and Schlag (1989) found neurons just lateral to MD in the central lateral, central superior lateralis and paracentralis nuclei that are close to our lateral band, as were neurons in the delayed-saccade task of Watanabe and Funahashi (2004). Tanaka (2007a,b) explored motor thalamus (VA and VL) and central thalamus, and some neurons therein might also have overlapped our band. In net, the saccade-related neurons in previous studies largely fall outside our lateral band in MD, but some neurons probably do overlap that lateral band. What we do not know is whether these overlapping neurons are CD neurons or serve other saccade-related functions.

In any case, we have identified the location of the saccade-related neurons consistent with CD signals, and we have provided the stereotaxic location for that band of neurons. This should provide the critical information for locating these neurons in future studies. In addition, our results provide the necessary information for comparing the location of CD neurons in the monkey with the recent identification in humans of a lateral area of MD with connections to the FEF using diffusion tensor imaging (Yao et al., 2019). In both monkey and humans, the area is at the lateral edge of MD, although it is somewhat lower on the lateral edge in our monkeys than in the human.

Relation of the CD circuit to schizophrenia

A possible relation between CD and schizophrenia was first suggested by Feinberg (1978). He suggested that a deficit in the functioning of CD in schizophrenic patients contributes to their lack of knowledge about whether or not they produced a particular action (referred to as a loss of agency). Sommer and Wurtz (2008) suggested that the CD circuit from SC through MD to FEF might provide the CD that Feinberg originally envisioned. Two studies in monkeys using partial inactivation of the CD in MD have shown deficits in behavior: in non-visually guided saccades using the double step task (Sommer and Wurtz, 2002, 2004b), and perceived location of saccade endpoints (Cavanaugh et al. 2016). Similar behavioral studies were then conducted in normal humans and in schizophrenic patients (for review, see Thakkar et al., 2017; Bansal et al., 2018), and deficits with similarities to those found in monkeys were found in these patients. In addition, the pathway between MD and FEF was found to be compromised in schizophrenic patients compared with human control subjects (Yao et al., 2019).

In summary, there are two behavioral studies that show deficits in monkeys with partial inacativation of a CD circuit in MD, and the same behavioral experiments show deficits in schizophrenic patients. In addition, there is a relay of a CD from MD to FEF in monkeys that is located at the lateral edge of MD, and there is a similar connection in humans also at the lateral edge of MD. This pathway appears to be compromised in schizophrenic patients. Thus, there are three suggestive comparisons between a CD circuit in monkeys and humans that support the possible role of a CD deficit in schizophrenic patients. The addition of information about the relay of the CD in MD thalamus and the location of that CD relay should contribute to understanding the thalamus, and possibly open a window on the mechanism underlying agency deficits in schizophrenic patients.

References

Bansal S, Ford JM, Spering M (2018) The function and failure of sensory predictions. Ann NY Acad Sci 1426:199–220.

Cavanaugh J, Berman RA, Joiner WM, Wurtz RH (2016) Saccadic corollary discharge underlies stable visual perception. J Neurosci 36:31–42.

Chen CY, Hoffmann KP, Distler C, Hafed ZM (2019) The foveal visual representation of the primate superior colliculus. Curr Biol 29:2109–2119.

Crapse TB, Sommer MA (2009) Frontal eye field neurons with spatial representations predicted by their subcortical input. J Neurosci 29:5308–5318.

Dubach MF, Bowden DM (2009) BrainInfo online 3D macaque brain atlas: a database in the shape of a brain. Society for Neuroscience Annual Meeting. Chicago. Abstract No. 199.5.

Erickson SL, Lewis DA (2004) Cortical connections of the lateral mediodorsal thalamus in cynomolgus monkeys. J Comp Neurol 473:107–127.

Feinberg I (1978) Efference copy and corollary discharge: implications for thinking and disorders. Schizophr Bull 4:636–640.

Goldman-Rakic PS, Porrino LJ (1985) The primate mediodorsal (MD) nucleus and its projection to the frontal lobe. J Comp Neurol 242:535–560.

Hallett PE, Lightstone AD (1976) Saccadic eye movements toward stimuli triggered by prior saccades. Vision Res 16:88–106.

Joiner WM, Cavanaugh J, FitzGibbon EJ, Wurtz RH (2013) Corollary discharge contributes to perceived eye location in monkeys. J Neurophysiol 110:2402–2413.

Jones EG (2007) The thalamus, Ed 2. Cambridge: Cambridge University Press.

Koyano KW, Machino A, Takeda M, Matsui T, Fujimichi R, Ohashi Y, Miyashita Y (2011) In vivo visualization of single-unit recording sites using MRI-detectable elgiloy deposit marking. J Neurophysiol 105:1380–1392.

Kunzle H (1976) Thalamic projections from the precentral motor cortex in Macaca fascicularis. Brain Res 105:253–267.

McAlonan K, Cavanaugh J, Wurtz RH (2008) Guarding the gateway to cortex with attention in visual thalamus. Nature 456:391–394.

Mohler CW, Wurtz RH (1976) Organization of monkey superior colliculus: intermediate layer cells discharging before eye movements. J Neurophysiol 39:722–744.

Paxinos G, Huang X, Toga AW (2000) The rhesus monkey brain in sterotaxic coordinates. San Diego: Academic Press.

Preuss TM, Goldman-Rakic PS (1987) Crossed corticothalamic and thalamocortical connections of macaque prefrontal cortex. J Comp Neurol 257:269–281.

Rath-Wilson K, Guitton D (2015) Oculomotor control after hemidecortication: a single hemisphere encodes corollary discharges for bilateral saccades. Cortex 63:232–249.

Rohlfing T, Kroenke CD, Sullivan EV, Dubach MF, Bowden DM, Grant KA, Pfefferbaum A (2012) The INIA19 template and NeuroMaps atlas for primate brain image parcellation and spatial normalization. Front Neuroinform 6:27.

Schlag-Rey M, Schlag J (1989) The central thalamus. In: The neurobiology of saccadic eye movements, reviews of oculomotor research (WurtzRH, GoldbergME, eds), pp 361–390. Amsterdam: Elsevier.

Schneider CA, Rasband WS, Eliceiri KW (2012) NIH Image to ImageJ: 25 years of image analysis. Nat Methods 9:671–675.

Sherman SM, Guillery RW (1996) Functional organization of thalamocortical relays. J Neurophysiol 76:1367–1395.

Sommer MA, Wurtz RH (2002) A pathway in primate brain for internal monitoring of movements. Science 296:1480–1482.

Sommer MA, Wurtz RH (2004a) What the brain stem tells the frontal cortex. I. Oculomotor signals sent from superior colliculus to frontal eye field via mediodorsal thalamus. J Neurophysiol 91:1381–1402.

Sommer MA, Wurtz RH (2004b) What the brain stem tells the frontal cortex. II. Role of the SC-MD-FEF pathway in corollary discharge. J Neurophysiol 91:1403–1423.

Sommer MA, Wurtz RH (2008) Brain circuits for the internal monitoring of movements. Annu Rev Neurosci 31:317–338.

Sparks DL (1986) Translation of sensory signals into commands for control of saccadic eye movements: role of primate superior colliculus. Physiol Rev 66:118–171.

Tanaka M (2007a) Cognitive signals in the primate motor thalamus predict saccade timing. J Neurosci 27:12109–12118.

Tanaka M (2007b) Spatiotemporal properties of eye position signals in the primate central thalamus. Cereb Cortex 17:1504–1515.

Thakkar NK, Diwadkar VA, Rolfs M (2017) Oculomotor prediction: a window into the psychotic mind. Trends in Cognitive Sciences 21:344–356.

Watanabe Y, Funahashi S (2004) Neuronal activity throughout the primate mediodorsal nucleus of the thalamus during oculomotor delayed-responses. I. Cue-, delay-, and response-period activity. J Neurophysiol 92:1738–1755.

Wurtz RH (2008) Neuronal mechanisms of visual stability. Vision Res 48:2070–2089.

Wurtz RH (2018) Corollary discharge contributions to perceptual continuity across saccades. Annu Rev Vis Sci 4:215–237.

Wurtz RH, Goldberg ME (1972) Activity of superior colliculus in behaving monkey: III. Cells discharging before eye movements. J Neurophysiol 35:575–586.

Wurtz RH, Albano JE (1980) Visual-motor function of the primate superior colliculus. Annu Rev Neurosci 3:189–226.

Yao B, Neggers SFW, Rolfs M, Rösler L, Thompson IA, Hopman HJ, Ghermezi L, Kahn RS, Thakkar KN (2019) Structural thalamofrontal hypoconnectivity is related to oculomotor corollary discharge dysfunction in schizophrenia. J Neurosci 39:2102–2113.